

# An adaptive safety layer with hard constraints for safe reinforcement learning in multi-energy management systems

Glenn Ceusters<sup>1,2,3,\*</sup>, Muhammad Andy Putratama<sup>2</sup>, Rüdiger Franke<sup>1</sup>, Ann Nowé<sup>3</sup>, Maarten Messagie<sup>2</sup>

<sup>1</sup> ABB, Hoge Wei 27, 1930 Zaventem, Belgium; glenn.ceusters@be.abb.com; ruediger.franke@de.abb.com;

<sup>2</sup> Vrije Universiteit Brussel (VUB), ETEC-MOBI, Pleinlaan 2, 1050 Brussels, Belgium; glenn.leo.ceusters@vub.be; muhammad.andy.putratama@vub.be, maarten.messagie@vub.be;

<sup>3</sup> Vrije Universiteit Brussel (VUB), AI-lab, Pleinlaan 2, 1050 Brussels, Belgium; gceusters@ai.vub.ac.be; ann.nowe@ai.vub.ac.be;

\* **Correspondence:** glenn.ceusters@be.abb.com

**Abstract:** Safe reinforcement learning (RL) with hard constraint guarantees is a promising optimal control direction for multi-energy management systems. It only requires the environment-specific constraint functions itself *a priori* and not a complete model (i.e., plant, disturbance and noise models, and prediction models for states not included in the plant model - e.g. demand forecasts, weather forecasts, price forecasts). The project-specific upfront and ongoing engineering efforts are therefore still reduced, better representations of the underlying system dynamics can still be learnt, and modelling bias is kept to a minimum (no model-based objective function). However, even the constraint functions alone are not always trivial to accurately provide in advance (e.g., an energy balance constraint requires the detailed determination of all energy inputs and outputs), leading to potentially unsafe behaviour. Furthermore, while computing the closest feasible action results in a high sample efficiency (as in `OptLayer`), it does not necessarily have a high utility (especially in the initial learning stage of RL agents). In contrast, providing a safe fallback policy *a priori* can lead to a high initial utility, but was shown to result in a poor sample efficiency and inability to include equality constraints (as in `SafeFallback`). In this paper, we present two novel advancements: (I) combining the `OptLayer` and `SafeFallback` method, named `OptLayerPolicy`, to increase the initial utility while keeping a high sample efficiency and the possibility to formulate equality constraints. (II) introducing self-improving hard constraints, to increase the accuracy of the constraint functions as more and new data becomes available so that better policies can be learnt. Both advancements keep the constraint formulation decoupled from the RL formulation, so new (presumably better) RL algorithms can act as drop-in replacements. We have shown that, in a simulated multi-energy system case study, the initial utility is increased to 92.4% (`OptLayerPolicy`) compared to 86.1% (`OptLayer`) and that the policy after training is increased to 104.9% (`GreyOptLayerPolicy`) compared to 103.4% (`OptLayer`) - all relative to a *vanilla* RL benchmark. Although introducing surrogate functions into the optimisation problem requires special attention, we conclude that the newly presented `GreyOptLayerPolicy` method is the most advantageous.

**Keywords:** reinforcement learning; surrogate optimisation; constraints; multi-energy systems; energy management system

## Highlights

- Increased initial utility while retaining a high sample efficiency
- Ability to self-improve the hard constraints
- Better policies can be found with more accurate constraints
- Constraint formulation remains decoupled from (optimal) control

## Nomenclature

### Sets

$\mathbb{R}$	Real numbers
$\mathbb{T}$	Time domain
$\mathbb{U}, A$	Action space
$\mathbb{U}_c$	Action constraints
$\mathbb{X}, S$	State space
$\mathbb{X}_c$	State constraints

### Symbols

$\eta$	Efficiency
$\gamma$	Discount factor, Binary variable
$\pi$	Policy
$C$	Cost
$c$	Constraint
$COP$	Coefficient of performance
$D$	Day of the week
$d$	Distance
$E\{\cdot\}$	Expectation
$H$	Hour of the day
$h$	Threshold
$J$	Objective
$L$	Loss
$n$	Amount
$P$	Electrical power
$P_a$	Transition probability
$Pr$	Probability
$Q$	Thermal power
$R$	Reward
$SOC$	State of charge
$T$	Temperature

$t$	Time
$u, a$	Action
$w$	Wiener process
$x, s$	State
$x, y$	Scalarisation weights
$X$	Price
$z$	Infeasibility cost

### Subscripts/Superscripts

'	next
<i>bess</i>	Battery energy storage system
<i>boil</i>	Boiler
<i>chp</i>	Combined heat and power
<i>cond</i>	Condenser
<i>el</i>	Electrical
<i>env</i>	Outdoor environment
<i>evap</i>	Evaporator
<i>hp</i>	Heat pump
<i>i</i>	initial
<i>j</i>	constraint index
<i>max</i>	Maximum
<i>min</i>	Minimum
<i>safe</i>	safe, feasible
<i>solar</i>	Photovoltaic system
<i>tess</i>	Thermal energy storage system
<i>th</i>	Thermal
<i>train</i>	Training (interval)
<i>wind</i>	Wind turbines

### Other symbols

$\bar{(\cdot)}$	Nominal, Average
$\hat{(\cdot)}$	Unknown
$\hat{(\cdot)}$	Predicted

## 1. Introduction

The possibility to integrate multiple energy, commodity, and utility streams is increasingly available as the energy technologies that allow for this sector coupling are more mature, more widely spread installed, and more creatively found. The overall system efficiency and performance can then be enhanced by implementing an integrated control strategy, that considers all energy assets across all energy carriers – including all sources of flexibility (i.e.,

storage, controllable loads) within all sub-systems. This seemingly limitless optimisation potential then typically has an economic or environmental-oriented objective [1] or has a combination of multiple, sometimes conflicting, objectives.

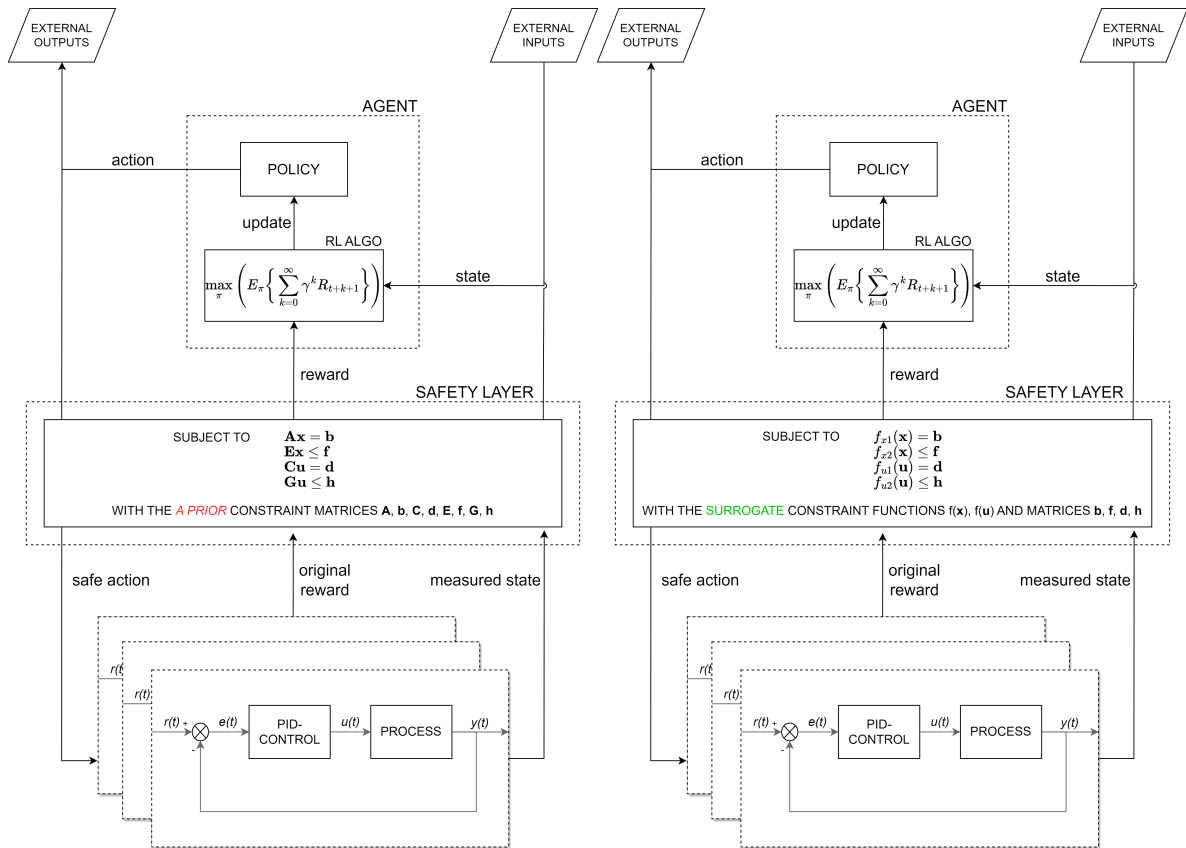
Finding an optimum or Pareto optimum level of operation for such multi-energy systems is no small task. It requires establishing and maintaining specific set-points to first ensure a disruptive-free operation by fulfilling all system constraints and secondary to pursue a desired objective (e.g., energy costs or  $CO_2$ -equivalent emissions minimisation) [2]. Moreover, the use of flexibilities introduces a dependency between successive time steps, which in theory requires an *infinite* horizon optimisation calculation. While managing multiple uncertainties (e.g., variation in demands, weather, and pricing) only leaves us with an *expectation* in these *continuous* systems.

In practice, model-predictive control (MPC) is often used as the optimal control technique as it has mature stability, feasibility, robustness, and constraint handling theory [3]. However, it does require a detailed model in advance (i.e., plant models, input and output disturbance models, measurement noise models and prediction models for states not included in the plant model - e.g., demand forecasts, weather forecasts, price forecasts) which is typically not adaptive [4]. In an attempt to overcome these shortcomings, reinforcement learning (RL) is model-free and inherently adaptive, yet has immature stability, feasibility, robustness, and constraint handling theory. It is only recently that [Ceusters \*et al.\*](#) [5] showed that a (near-to) optimal multi-energy management policy can be learnt safely. Hereby, the project-specific upfront and ongoing engineering efforts remain reduced, a better representation of the underlying system dynamics can still be learnt, and modelling bias is kept to a minimum (no model-based objective function).

### 1.1. Problem statement

However, even the constraint functions themselves (see [Figure 1a](#)) are not always trivial to provide accurately in advance (e.g., see the energy balance constraint [Equation 9d](#)) – especially when auxiliary state variables are required or when they need to be activated under particular conditions [6]. Even when they could be given in advance, they may not continue to be sufficiently accurate over time (e.g., efficiency decay). Furthermore, while computing the closest feasible action results in a high sample efficiency (as in OptLayer [6]), it does not necessarily have a high utility (especially in the initial learning stage of RL agents). In contrast, providing a safe fallback policy *a priori* can lead to a high initial utility, but was shown to result in a poor sample efficiency and the inability to include equality constraints (as in SafeFallback [5]).

Our goal, therefore, is not only to ensure that *every* interaction with the underlying environment (a multi-energy system in our case study) is safe by satisfying to a set of constraints. But also to improve the accuracy of the constraints themselves (see [Figure 1b](#)), as more data becomes available, to improve the initial utility and keep a high sample efficiency while the constraint handling remains independent of the (optimal) control technique. This is so that future, presumably better, yet inherently unsafe, optimisation algorithms (e.g., a new RL algorithm) can act as drop-in replacements.



(a) *vanilla* shielded (safe) reinforcement learning    (b) *grey* shielded (safe) reinforcement learning

**Figure 1.** Block diagram representation: the actions of the RL agent, when in a specific state, are checked for feasibility by evaluating them against a set of, either *a priori* or *surrogate*, constraint functions. These functions then serve as a safety layer measure to protect the environment from unsafe control actions. It is important to note that we assume that the continuous handling of unconstrained errors (which involves minimising the difference between a desired set-point and a measured process variable) is carried out by proportional-integral-derivative (PID) controllers.

## 1.2. Contribution and outline

Our contributions presented in this work are, to the best of the authors' knowledge, believed to be the first of their kind, and can be outlined as follows:

- Combining the OptLayer [6] and SafeFallback [5] method, named OptLayerPolicy, to increase the initial utility while keeping a high sample efficiency and the possibility to formulate equality constraints.
- Introducing self-improving (adaptive) hard constraints, to increase the accuracy of the constraint functions as more and new data becomes available so that better policies can be learnt.

In [section 2](#) we have a concise discussion of related work, [section 3](#) introduces the proposed methodologies, while [section 4](#) presents the case study specific toolchain, multi-energy system simulation environment, safety layer, RL agent, and evaluation

procedure. Finally, [section 5](#) discusses the results and provides directions for future work so that [section 6](#) presents our conclusion. In [Appendix A](#) we show time series visualisations of the self-discovered policies, in [Appendix B](#) the full learning and cost curves for the agents assessed in the case study, in [Appendix C](#) the pseudocode and hyperparameters of the specific RL agent (TD3, i.e., Twin Delayed Deep Deterministic Policy Gradient) and in [Appendix D](#) the run-time statistics.

## 2. Related work

Reinforcement learning has been proposed and demonstrated for a wide variety of applications in power and energy systems, as extensively reviewed by e.g. [Cao et al. \[7\]](#), [Yang et al. \[8\]](#) and [Perera and Kamalaruban \[9\]](#), and even for multi-energy systems more specifically by [Zhou \[10\]](#). It ranges from real-time control (e.g., robust voltage control by [Petruşev et al. \[11\]](#)) to energy management systems (EMS) RL applications. Recent EMS examples include, [Zhou et al. \[12\]](#) who proposed deep RL for the stochastic EMS of a multi-energy system and introduced a prioritised experience relay that improves the training efficiency and thus the convergence rate of the RL algorithm. While a multi-agent deep RL EMS, using multi-agent counterfactual soft actor-critic (mCSAC [13]), was demonstrated by [Zhu et al. \[14\]](#) in a simulated multi-energy industrial park, by [Ahrarinouri et al. \[15\]](#) using multi-agent Q-learning in a simulated distributed and interconnected multi-carrier energy hub case study, and by [Jendoubi and Bouffard \[16\]](#) using multi-agent Deep Deterministic Policy Gradient (MADDPG) in separate simulated microgrid, eco-neighbourhood and flat building case studies. [Ceusters et al. \[4\]](#), furthermore, benchmarked an on- and off-policy multi-objective model-free deep RL algorithm against a linear MPC on two separate simulated multi-energy systems and showed that the RL agent, using soft constraints, can outperform the MPC (since it learnt a better representation of the *true* system dynamics). [Sun et al. \[17\]](#) then also demonstrated a multi-objective deep RL approach with soft constraints yet on an IEEE-30 node optimal power flow problem. However, using RL, without adequate measures, could result in undesirable specific losses (e.g., monetary, comfort) and, in extreme cases, in human harm. This as, RL inherently requires the interaction with its environment - and does this without the consideration of any constraints (besides the limits of the action space itself). As also reported by [Ceusters et al. \[5\]](#), most works knowingly (and therefore reported as such) or unknowingly, either neglected these environment-specific constraints or greatly simplified them - limiting their real-world use. Safe RL, therefore, aims to: "*learn policies that maximise the expectation of the return in problems in which it is important to ensure reasonable system performance and/or respect safety constraints during the learning and/or deployment processes*" - as defined by [García and Fernández \[18\]](#). Then [Ceusters et al. \[5\]](#) were one of the first to show that a (near-to) optimal multi-energy management policy can be learnt safely with hard constraints, that these constraints can be formulated independently of the (optimal) control technique, and that better policies can be found starting from an initial safe fallback policy. While [Feng et al. \[19\]](#) introduced a robust state generation procedure in combination with a dynamic pricing mechanism to economically dispatch an industrial park using a variation of the distributed proximal policy optimisation (DPPO) algorithm subject to a set of hard constraints to ensure safe (near-to) optimal operation. However, even only assuming the availability of perfectly accurate constraint functions themselves is not always possible – especially when auxiliary

state variables are required or when they need to be activated under particular conditions, as also needed by OptLayer [6] which is considered a current state-of-the-art benchmark.

On the other hand, more traditional optimisation approaches - typically in a receding horizon control manner (e.g., model-predictive control), still see significant advancements for the management of multi-energy systems. Recent examples include: [Zhu et al. \[20\]](#) who designed a joint multi-energy scheduling and trading algorithm based on Lyapunov optimisation and a double-auction mechanism. Simulations based on real data showed that individual microgrids could achieve a time-averaged profit that was arbitrarily close to an optimum value while avoiding compromising their own comfort. [Zhu et al. \[21\]](#) then later employed a fast distributed algorithm based on stochastic gradient descent with a two-timescale implementation to address energy storage constraints and short-term balancing. In addition, they estimated users' willingness to shift their load, who participated in an incentive mechanism to reduce peak loads. Analytical and numerical results showed that when the bid-ask spread of electricity was sufficiently small, the proposed algorithm could achieve cost levels close to optimal asymptotically. Also, [Zou et al. \[22\]](#) introduced a two-tiered peer-to-peer (P2P) multi-energy trading system for an interconnected distribution network (DN) and district heating network (DHN). In the lower tier, nodal agents optimised energy schedules and P2P trading strategies using Nash bargaining theory. In the upper tier, operators minimised power losses and ensured network constraints by reconfiguring the DN and DHN and adjusting trades as needed. The DN operation was modelled using a linearised DistFlow model with radiality constraints, while the DHN employed a quasi-linear thermal flow model. The framework's effectiveness was demonstrated on an IEEE 33-bus DN and a 23-node DHN. And as a final example, [Zou et al. \[23\]](#) introduced an energy management method for a multi-energy microgrid (MEMG), that employed the transactive energy concept and formulated the problem as a Stackelberg game-theoretic bi-level optimisation model. This approach formed a day-ahead stochastic mixed-integer linear program (MILP) and an intra-day deterministic model. To solve these models, an adaptive Progressive Hedging algorithm decomposed the day-ahead stochastic MILP into scenario-based subproblems that could be solved in parallel. Meanwhile, an outer approximation algorithm was employed in the intra-day stage to linearise the bi-linear objective function. Nevertheless, it is clear that these approaches require highly detailed mathematical formulations *a priori* (i.e., plant models, input and output disturbance models, measurement noise models and prediction models for states not included in the plant model - e.g., demand forecasts, weather forecasts, price forecasts), which are typically not adaptive and which are not all required with safe RL [4].

Considering a broader view across both the RL research space and the control theory space, [Brunke et al. \[24\]](#) provided a safe learning review and showed: (1) approaches that learn uncertain system dynamics and safely improve the policy starting with an imperfect *a priori* dynamic model, (2) approaches that do not have a model or even constraints in advance and encourage safety or robustness (e.g., by penalising dangerous actions) but provide no strict guarantees, and (3) approaches that provide safety certificates to inherently unsafe learning-based controllers, using an *a priori* dynamic model. Hence, there are multiple approaches to safe (reinforcement) learning that exist, varying in their level of safety. These approaches can be categorised as follows, in ascending order of safety: soft-constraint

satisfaction, chance-constraint satisfaction, and hard-constraint satisfaction. Recent examples – one of each category – include, [McKinnon and Schoellig \[25\]](#) who proposed a stochastic MPC, where the predicted cost, using a computationally efficient yet expressively limited *a priori* dynamic model, is corrected by a simple learnt dynamics model over the MPC horizon. [Bharadhwaj et al. \[26\]](#) who extended Conservative Q-Learning (CQL) towards Conservative Safety Critic (CSC) and showed safety constraint satisfaction with *high probability* while providing provable safe policy improvements. And finally, [Lopez et al. \[27\]](#) who introduced robust adaptive control barrier functions (CBF) which allowed safe adaptation of structured parametric uncertainties in the time derivatives of CBFs which are used together with an inherently unsafe adaptive control algorithm.

Nevertheless, a model-free safe RL approach of the following *combined* characteristics has – to the best of the authors' knowledge – never been proposed: (i) providing hard-constraints satisfaction guarantees (ii) while decoupled from the RL (as a Markov Decision Process) formulation, (iii) both during training a (near) optimal policy (involving exploratory and exploitative steps) as well as during the deployment of any policy (e.g., offline pre-trained RL agents) and (iv) this while learning uncertain constraint components and safely improving the policy with high sample efficiency, and (v) starting from an increased initial utility, to (vi) demonstrate for the energy management of multi-energy systems.

### 3. Proposed methodology

We start from a discrete time-varying stochastic system and recognise that this is an approximation for continuous<sup>1</sup> systems, in the form of:

$$x_{t+1} = f_t(x_t, u_t, w_t) \quad (1)$$

where  $x_t$  is the  $n$ -dimensional *state* vector, which is an element of the *state space*  $\mathbb{X}$ , and  $u_t$  the  $m$ -dimensional *control* or *action* vector, which is an element of the input or *action space*  $\mathbb{U}$ , and  $w_t$  a Wiener process, i.e. some stochastic noise, that – with this formulation – can enter the dynamics in any form. The problem is to find a control signal  $u_t = \pi_t(x_t)$ , with  $\pi$  being the control *policy*, so that the infinite-horizon, yet discounted (if  $\gamma^t < 1$ ), cost function from [Görges \[3\]](#) in a unified notation

$$C(x_i, u_t) = E \left\{ \sum_{t=0}^{\infty} \gamma^t L_t(x_t, u_t, w_t) \right\} \quad (2)$$

is minimal, where  $L_t(x_t, u_t, w_t)$  is the stage *loss*. Considering the inherently stochastic nature of the system described by [Equation 1](#), one can only strive to minimise the *expectation*  $E\{\cdot\}$  of the corresponding cost function across the multitude of stochastic trajectories originating from  $x_i$ . This results in the discounted infinite-horizon objective function, again from [Görges \[3\]](#) in unified notation:

---

<sup>1</sup> as we assume that the continuous error handling is performed by well-tuned PID-controllers

$$J_\infty(x_t) = \min_{u_t \in \mathcal{U}_t} \left( E \left\{ \sum_{t=0}^{\infty} \gamma^t L_t(x_t, u_t, w_t) \right\} \right), \forall x_t \quad (3)$$

Following the standard RL formulation of the state-value function from [Sutton and Barto \[28\]](#), the objective is to find a policy  $\pi$ , which is a mapping of states,  $s = x$ , to actions,  $a = u$ , that maximises an expected sum of discounted rewards, yet making it subject to the constraints,  $c$ :

$$\max_{\pi} \left( E_{\pi} \left\{ \sum_{k=0}^{\infty} \gamma^k R_{t+k+1} \right\} \right) \quad (4a)$$

$$\text{s.t. } s_t = s \quad t \in \mathbb{T}_0^{+\infty} \quad (4b)$$

$$c_t^j(s_t, a_t, w_t) \leq 0 \quad t \in \mathbb{T}_0^{+\infty}, j \in \mathbb{R}_1^{n_c} \quad (4c)$$

where  $E_{\pi}$  is the expected value, following the policy  $\pi$ , of the rewards  $R$  and reduced with the discount factor  $\gamma$  over an infinite sum at any time step  $t$  with  $n_c$  amount of constraint functions.

Note that [Equation 4a](#) corresponds to a stochastic optimal control problem with an infinite time horizon in discrete time. It can be regarded as the time-invariant version of [Equation 3](#), where  $R_t = -L_t(x_t, u_t, w_t)$ . However, it diverges from the standard formulation of RL due to the subjection of hard-constraint functions,  $c_t^j$ . This can include *state constraints*  $\mathbb{X}_c \in \mathbb{X}$ , *action* or *input constraints*  $\mathbb{U}_c \in \mathbb{U}$  and *stability guarantees* (e.g., Lyapunov, asymptotic or exponential stability). Rather than proposing a specific safe RL algorithm, we propose to decouple the constraint function formulation from the (RL) agent so that any (new RL) algorithm can be used – while always guaranteeing hard-constraint satisfaction and this in a minimally invasive way (i.e., correcting actions to the closest possible feasible action).

### 3.1. OptLayerPolicy method

The minimal invasive correction of predicted actions,  $\tilde{a}$ , e.g. originating from a RL algorithm, can be expressed from [Pham et al. \[6\]](#) (i.e., the original OptLayer formulation) as:

$$a_{safe,t} = \arg \min_{a_t} \frac{1}{2} \| a_t - \tilde{a}_t \|^2 \quad (5a)$$

$$\text{s.t. } c_t^j(s_t, a_t, w_t) \leq 0 \quad t \in \mathbb{T}_0^{+\infty}, j \in \mathbb{R}_1^{n_c} \quad (5b)$$

which is a Quadratic Program (QP), where  $a_t$  is the optimisation variable that results in the closest feasible safe action  $a_{safe}$ , which does not affect the optimality as  $a_t$  does not depend on  $\tilde{a}_t$  [6]. The distance closest to the possible feasible action is then simply:

$$d_{safe,t} = \min_{a_t \in \mathbb{R}^{n_c}} \frac{1}{2} \| a_t - \tilde{a}_t \|^2 \quad (6)$$

While this is the closest distance for a minimally invasive correction, this does not necessarily result in a close-to-optimal action. We, therefore, propose to fallback on an *a priori* safe policy,  $\pi^{safe}$  (i.e., as in the SafeFallback [5] algorithm), when the distance,  $d_{safe}$ , surpasses a given threshold  $h_{safe}$ . This safe fallback policy can typically be derived through classic control theory in the form of a set of hard-coded rules such as a simple rule-based policy (e.g., a priority-based energy management strategy - which is commonly available or easily constructable - see subsection 4.4 for the safe fallback policy of the considered case study).

While this relies on the utility of the (non-optimal) safe fallback policy itself, we will later show its effectiveness. The OptLayerPolicy algorithm is shown in algorithm 1.

---

**Algorithm 1: OptLayerPolicy**


---

```

1 Input: initialise RL algorithm, initialise constraint functions in sets  $\mathbb{X}_c$  and  $\mathbb{U}_c$ ,
   initialise safe fallback policy  $\pi^{safe}$ 
2 for  $k = 0, 1, 2, \dots$  do
3   Observe state  $s$  and predict action  $\tilde{a}$ 
4   Compute safety distance  $d_{safe}$ 
5   if  $d_{safe} \leq h_{safe}$  then
6      $a_{safe} = \arg \min_{a_t} \frac{1}{2} \| a_t - \tilde{a}_t \|^2 \quad s.t. \quad c_t^j(s_t, a_t, w_t) \leq 0$ 
7   else
8      $a_{safe} = \pi^{safe}(s)$ 
9   end
10  Execute  $a_{safe}$  in the environment
11  Observe next state  $s'$ , reward  $r$  and done signal  $d$  to indicate whether  $s'$  is terminal
12  Give experience tuple  $(s, a_{safe}, r, s', d)$  and if  $a_{safe} \neq \tilde{a} : (s, \tilde{a}, r - z, s', d)$  with cost  $z$ 
13  if  $s'$  is terminal, reset environment state
14 end

```

---

### 3.2. GreyOptLayerPolicy method

We can improve the initial utility of the *vanilla* RL agent, by using a safe fallback policy when a predicted unsafe action is too far from the feasible solution space (i.e., under the notion that random<sup>2</sup> safe actions have a low utility) - as outlined in the previous section. However, all constraint functions (Equation 5b) are assumed to be *true*. In reality, we typically only have access to a nominal set of constraints with an *a priori* unknown error (e.g., see Equation 9d and Table 2). We can express this from Brunke *et al.* [24] for constraint functions as:

$$c_t^j(s_t, a_t, w_t) = \bar{c}_t^j(s_t, a_t) + \hat{c}_t^j(s_t, a_t, w_t) \quad (7)$$

where  $(\bar{\cdot})$  is the nominal component, reflecting our prior knowledge, and  $(\hat{\cdot})$  is an unknown component, that can be learnt from data - making the equation and therefore the approach *adaptive*. The GreyOptLayerPolicy algorithm then becomes:

---

<sup>2</sup> as RL agents typically have an initial random exploration phase

**Algorithm 2:** GreyOptLayerPolicy

---

```

1 Input: initialise RL algorithm, initialise nominal constraint functions  $\tilde{c}_t^j$  in sets  $\mathbb{X}_c$  and
    $\mathbb{U}_c$ , initialise supervised learning models for  $\hat{c}_t^j$ , initialise safe fallback policy  $\pi^{safe}$ 
2 for  $k = 0, 1, 2, \dots$  do
3   Observe state  $s$  and predict action  $\tilde{a}$ 
4   Compute safety distance  $d_{safe}$ 
5   if  $d_{safe} \leq h_{safe}$  then
6      $a_{safe} = \arg \min_{a_t} \frac{1}{2} \| a_t - \tilde{a}_t \|^2 \quad s.t. \quad \tilde{c}_t^j(s_t, a_t) + \hat{c}_t^j(s_t, a_t, w_t) \leq 0$ 
7   else
8      $a_{safe} = \pi^{safe}(s)$ 
9   end
10  Execute  $a_{safe}$  in the environment
11  Observe next state  $s'$ , reward  $r$  and done signal  $d$  to indicate whether  $s'$  is terminal
12  Give experience tuple  $(s, a_{safe}, r, s', d)$  and if  $a_{safe} \neq \tilde{a} : (s, \tilde{a}, r - z, s', d)$  with cost  $z$ 
13  if  $k \bmod h_{train} = h_{train} - 1$  then
14    fit  $\hat{c}_t^j$  using supervised learning with buffer of  $(s, a_{safe})$ 
15  end
16  if  $s'$  is terminal, reset environment state
17 end

```

---

where  $h_{train}$  is the training interval for fitting the *a priori* unknown components of the constraints (see subsection 4.4 for the specifics of our case study). However, this introduces function approximators (e.g., artificial neural networks) into the optimisation problem (Equation 5a) – which are not trivial to integrate when using exact solving methods. Nevertheless, Gunnell *et al.* [29] recently integrated multiple machine learning algorithms in a gradient descent optimisation framework - which is also the framework used in this work (i.e., GEKKO [30]).

## 4. Case study

### 4.1. Toolchain

We use a multi-energy systems simulation model, that first was developed by Ceusters *et al.* [4] and later modified by Ceusters *et al.* [5]. This allowed for the consequence-free verification of the safe operation (i.e., with no risk of violating real-life constraints with its potential loss of comfort or, in extreme cases, human harm). The presumed to be *true* multi-physical first-principle equations were developed in Modelica [31] due to its object-oriented nature and the availability of highly specialised libraries and elementary components. To allow for the exchange across different simulation environments and programming languages, this dynamic system model was exported as a co-simulation *functional mock-up unit* (FMU), as also proposed by Gräber *et al.* [32] and then wrapped in an OpenAI gym [33] in Python. The mixed-integer quadratic problem in the safety layer was formulated with GEKKO [30], as it allowed for the integration of machine learning algorithms

(used for  $\hat{\cdot}$  in Equation 7) into an exact optimisation framework. We have used Scikit-learn [34] for the supervised learning models of  $\hat{c}_i^j$ . The toolchain architecture is shown in Figure 2.

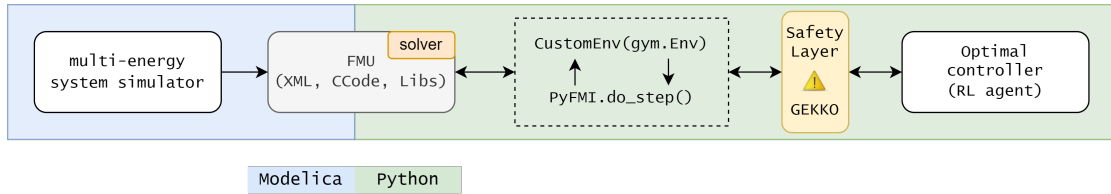


**Figure 2.** Toolchain architecture. Note that we used the `do_step()` method in PyFMI [35] over `simulate()` due to the significant reduction in run-time when initialised correctly, and also note that the Differential Algebraic Equations solver is part of the co-simulation FMU.

#### 4.2. Simulation model

The simulated multi-energy system, from Ceusters *et al.* [5], has the following topology:

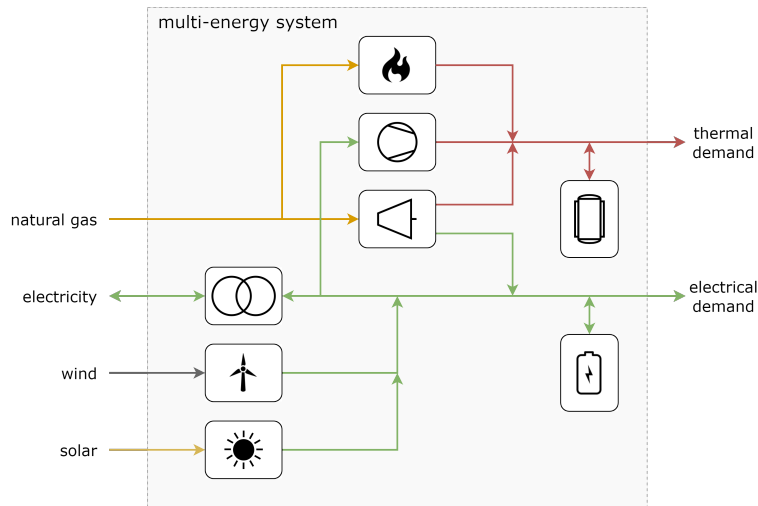


**Figure 3.** Topology of the multi-energy system simulation model.

The energy assets, listed here in order from left to right and top to bottom, are as follows: an electric grid connection, a wind turbine, a photovoltaic (PV) installation, a natural gas boiler, a heat pump (HP), a combined heat and power (CHP) unit, a thermal energy storage system (TESS) and a battery energy storage system (BESS). The dimensions of the considered multi-energy system are summarised in Table 1.

**Table 1.** Dimensions used in the multi-energy system simulation model.

Energy asset	Input	Output	$P_{nom}$	$P_{min}$	$E_{nom}$
grid connection	elec	elec	$+\infty$	$-\infty$	
wind turbine	wind	elec	$0.8 \text{ MW}_e$	1.5 %	
solar PV	solar	elec	$1.0 \text{ MW}_e$	0 %	
boiler	$\text{CH}_4$	heat	$2.0 \text{ MW}_{th}$	10 %	
heat pump	elec	heat	$1.0 \text{ MW}_{th}$	25 %	
CHP	$\text{CH}_4$	heat	$1.0 \text{ MW}_{th}$	50 %	
	$\text{CH}_4$	elec	$0.8 \text{ MW}_e$	50 %	
TESS	heat	heat	$+0.5 \text{ MW}_{th}$	$-0.5 \text{ MW}_{th}$	3.5 MWh
BESS	elec	elec	$+0.5 \text{ MW}_e$	$-0.5 \text{ MW}_e$	2.0 MWh

As also reported by [Ceusters et al. \[5\]](#), the simulation model is a detailed system of differential-algebraic equations (2.548 equations with an equal number of variables). However, it does not include any simulated control system (e.g., including PID controllers). Although we acknowledge the simplification, we make an abstraction of this control layer for this case study. The resulting control error is approximately 5%, as determined by [Ceusters et al. \[5\]](#) with separate simulations using a reduced discrete-time control horizon (5 seconds compared to 15 minutes, without any continuous *error* handling). This assumption is the same for every energy management algorithm considered, so the comparison remains valid. We furthermore deliberately will not use exactly the same equations in the safety layer as in the more detailed simulation model, to better mimic a real multi-energy management case study that always will have a remaining modelling error (caused by unknown parameters, inaccurate equations, or assets not working according to specifications - according to [Drgoña et al. \[36\]](#)).

#### 4.3. Safety layer

Starting from minimum and maximum electrical and thermal power output constraints:

$$Q_{boil}^{min} \times \gamma_{boil}^t \leq Q_{boil}^t \leq Q_{boil}^{max} \times \gamma_{boil}^t \quad \forall t, \gamma_{boil}^t \in \{0, 1\} \quad (8a)$$

$$\begin{bmatrix} Q_{hp}^{min} \\ P_{hp}^{min} \end{bmatrix} \times \gamma_{hp}^t \leq \begin{bmatrix} Q_{hp}^t \\ P_{hp}^t \end{bmatrix} \leq \begin{bmatrix} Q_{hp}^{max} \\ P_{hp}^{max} \end{bmatrix} \times \gamma_{hp}^t \quad \forall t, \gamma_{hp}^t \in \{0, 1\} \quad (8b)$$

$$\begin{bmatrix} Q_{chp}^{min} \\ P_{chp}^{min} \end{bmatrix} \times \gamma_{chp}^t \leq \begin{bmatrix} Q_{chp}^t \\ P_{chp}^t \end{bmatrix} \leq \begin{bmatrix} Q_{chp}^{max} \\ P_{chp}^{max} \end{bmatrix} \times \gamma_{chp}^t \quad \forall t, \gamma_{chp}^t \in \{0, 1\} \quad (8c)$$

$$Q_{tess}^{min} \leq Q_{tess}^t \leq Q_{tess}^{max} \quad \forall t \quad (8d)$$

$$P_{bess}^{min} \leq P_{bess}^t \leq P_{bess}^{max} \quad \forall t \quad (8e)$$

where  $Q^t$  and  $P^t$  are the thermal and electrical powers respectively (in accordance with [Table 1](#)) and  $\gamma^t$  binary variables that turn on/off the given asset (i.e., as their minimal powers are not zero). Furthermore, we assume a sufficiently large grid connection so that the electrical energy balance is always fulfilled. By doing so, we focus on satisfying the thermal energy balance and no additional constraints are considered in this case study (e.g., minimal run-and downtime, ramping rates). Writing out the thermal energy balance then becomes:

$$Q_{production}^t = Q_{demand}^t \quad \forall t \quad (9a)$$

$$Q_{boil}^t + Q_{hp}^t + Q_{chp}^t + Q_{tess}^t = Q_{demand}^t \quad \forall t \quad (9b)$$

$$\begin{aligned} & a_{boil}^t \cdot \eta_{boil}^t \cdot Q_{boil}^{max} + a_{hp}^t \cdot \frac{COP_{hp}^t}{COP_{hp}^{max}} \cdot Q_{hp}^{max} \\ & + a_{chp}^t \cdot \eta_{chp}^{t,th} \cdot Q_{chp}^{max} + a_{tess}^t \cdot f(SOC_{tess}^t) = Q_{demand}^t \quad \forall t \end{aligned} \quad (9c)$$

$$\begin{aligned} & a_{boil}^t \cdot f(T_{boil}^t) \cdot Q_{boil}^{max} + a_{hp}^t \cdot \frac{f(T_{evap}^t, T_{cond}^t)}{COP_{hp}^{max}} \cdot Q_{hp}^{max} \\ & + a_{chp}^t \cdot f(P_{chp}^t, Q_{chp}^t, T_{env}^t) \cdot Q_{chp}^{max} + a_{tess}^t \cdot f(\overline{T_{tess}^t}) = Q_{demand}^t \quad \forall t \end{aligned} \quad (9d)$$

where  $a$  are the (control) actions,  $\eta$  the energy efficiencies,  $COP$  the coefficient of performance,  $SOC$  the state of charge, and  $T$  various specific temperatures (i.e.,  $T_{boil}^t$  the return temperature to the boiler,  $T_{evap}^t$  the evaporator temperature of the heat pump,  $T_{cond}^t$  the condenser temperature of the heat pump,  $T_{env}^t$  the environmental air temperature and  $\overline{T_{tess}^t}$  the average temperature in the stratified hot water storage tank). However, the different functions  $f(\cdot)$  from Equation 9d are typically not trivial to *model* accurately. Our nominal models ( $\bar{\cdot}$ ) in Equation 7, which are also those used in Equation 5b, have the following metrics:

**Table 2.** Safety layer: nominal modelling metrics. Mean Absolute Error (MAE), Normalised Mean Absolute Error (NMAE) by range, i.e.,  $NMAE = MAE / \text{range}(\text{actual values})$

Energy asset	R2-score	MAE	NMAE
boiler	99.70%	20.00 kW	0.90%
heat pump	97.05%	36.04 kW	3.64%
CHP	99.77%	4.20 kW	0.35%
TESS	85.64%	39.52 kW	4.18%

In our nominal models, we have assumed a linear time-invariant relationship between the (control) action and the thermal power for the boiler and the CHP, yet a third-degree polynomial for the TESS and a second-degree polynomial for the heat pump – both also time-invariant. We note from Table 2 that the main improvement can be made in the heat pump and thermal energy storage functions, and therefore we have only included an adaptive component for these two assets:

$$\hat{Q}_{hp}^t = f(a_{hp}^t, Q_{hp}^{t-1}) \quad (10a)$$

$$\hat{Q}_{tess}^t = f(a_{tess}^t, SOC_{tess}^t, Q_{tess}^{t-1}, Q_{demand}^{t-1}) \quad (10b)$$

where  $Q_{hp}^{t-1}$  is the thermal power of the heat pump,  $Q_{tess}^{t-1}$  of the thermal energy storage system, and  $Q_{demand}^{t-1}$  of the thermal demand, all one time step before (i.e., historical lag features, as is common practice due to high autocorrelation). We use Multi-layer Perceptron (MLP) regressors from Scikit-learn [34] with ([15,10,10,10]) as the architecture of hidden layers for Equation 10a and [25, 20, 20, 10] for Equation 10b all with ReLU activation functions, using the Adam [37] solver and an adaptive learning rate. The total modelling metrics (nominal + unknown component) are given in Figure 6, using a training interval  $h_{train}$  of 1 week (672 time steps) in the first month and a monthly interval (2,688 time steps) thereafter.

#### 4.4. Safe fallback policy

The *a priori* safe fallback policy  $\pi^{safe}$ , can be *any* (non-optimal) policy that satisfies the constraints and can typically be provided by domain experts. In our case study, this is a simple priority/cascade rule, as in Ceusters *et al.* [5] and given by algorithm 3. Note that for clarity concerns, it is written in terms of thermal power output, yet it is still converted to actions  $a_{chp}^t$  and  $a_{boil}^t$  as going from Equation 9b to Equation 9c.

---

**Algorithm 3: safe fallback policy [5]**


---

```

if  $Q_{demand}^t < Q_{chp}^{min}$  then
  |  $Q_{chp}^t = 0$ 
  |  $Q_{boil}^t = Q_{demand}^t$ 
else
  | if  $Q_{demand}^t < Q_{chp}^{max}$  then
  | |  $Q_{chp}^t = Q_{demand}^t$ 
  | |  $Q_{boil}^t = 0$ 
  | else
  | |  $Q_{chp}^t = Q_{chp}^{max}$ 
  | |  $Q_{boil}^t = Q_{demand}^t - Q_{chp}^{max}$ 
  | end
end
end

```

---

#### 4.5. Energy managing RL agent

We formulate the energy managing RL agent as a fully observable discrete-time Markov Decision Process (MDP) with the tuple  $\langle S, A, P_a, R_a \rangle$  so that:

$$S^t = (E_{th}^t, E_{el}^t, P_{wind}^t, P_{solar}^t, X_{el}^t, SOC_{tess}^t, SOC_{bess}^t, H^t, D^t) \quad S^t \in S \quad (11a)$$

$$a_{boil}^t = (0, a_{boil}^{min} \rightarrow a_{boil}^{max}) \quad a_{boil}^t \in A \quad (11b)$$

$$a_{hp}^t = (0, a_{hp}^{min} \rightarrow a_{hp}^{max}) \quad a_{hp}^t \in A \quad (11c)$$

$$a_{chp}^t = (0, a_{chp}^{min} \rightarrow a_{chp}^{max}) \quad a_{chp}^t \in A \quad (11d)$$

$$a_{tess}^t = (a_{tess}^{min} \rightarrow a_{tess}^{max}) \quad a_{tess}^t \in A \quad (11e)$$

$$a_{bess}^t = (a_{bess}^{min} \rightarrow a_{bess}^{max}) \quad a_{bess}^t \in A \quad (11f)$$

$$P_a(s, s') = Pr(s_{t+1} = s' \mid s_t = s, a_t = a) \quad (11g)$$

$$R_a(s, s') = -(x \times L_{cost}^t + y \times L_{comfort}^t) - z \quad (11h)$$

where  $E_{th}^t$  is the thermal demand,  $E_{el}^t$  the electrical demand,  $P_{wind}^t$  the electrical wind in-feed,  $P_{solar}^t$  the electrical solar in-feed,  $X_{el}^t$  the electrical price signal,  $SOC_{tess}^t$  the state-of-charge (SOC) of the TESS,  $SOC_{bess}^t$  the SOC of the BESS,  $H^t$  the hour of the day and  $D^t$  the day of the week all at the  $t$ -th step, which constitute the state-space  $S$ . The action space  $A$  includes the control set-points from,  $a_{boil}^t$  the natural gas boiler,  $a_{hp}^t$  the heat pump,  $a_{chp}^t$  the CHP unit,  $a_{tess}^t$  the TESS, and  $a_{bess}^t$  the BESS all between the minimum and maximum power rates in accordance with [Table 1](#). Moreover,  $P_a$  signifies a transition probability, that exclusively relies on the current state and is unaffected by prior states (in other words, adhering to the Markov Property), for when the system is in a specific state  $s \in S$  at time step  $t$  and takes action  $a \in A$ , which would result in the system being in state  $s' \in S$  at the subsequent time step  $t + 1$ .

We formulate the objective, that is, the reward function, so that when maximising this function (via [Equation 4a](#)) we minimise the positive version of that function. Hence, we

minimise the energy costs  $L_{cost}^t$  in EUR and the loss in (thermal) comfort  $L_{comfort}^t = |Q_{demand}^t - Q_{production}^t|$  in Watt with scalarisation weights  $x = 1/10$  and  $y = 1/5e5$  and with an additional cost  $z = 1$  to further shape the reward when the original, uncorrected, predicted action  $\tilde{a}$  was *expected* to violate constraints. The loss in (thermal) comfort,  $L_{comfort}^t$ , serves as an additional fine-tuning mechanism to further mitigate the modelling error of the constraints itself (see [Table 2](#)), i.e., to further shape the reward and thus guide the agent towards safer actions. The discrete-time control horizon is 15 minutes. The state-space  $S$  is normalised and all actions in the action-space  $A$  are scaled between  $[+1, -1]$ .

As the specific RL algorithm, we use a twin delayed deep deterministic policy gradient agent (TD3, that is, twin delayed DDPG) from the `stable baseline` [38] implementations. The pseudocode and the used hyperparameters of the TD3 algorithm are given in [Appendix C](#).

#### 4.6. Evaluation

We evaluate our methods, `OptLayerPolicy` and `GreyOptLayerPolicy`, against a *vanilla* RL agent (i.e., without a safety layer and therefore being unsafe), the original `OptLayer` from [Pham et al.](#) [6] and the original `SafeFallback` from [Ceusters et al.](#) [5] (both as state-of-the-art benchmarks), in a week-long evaluation environment while having a separate year-long training environment using the simulation model as discussed in [subsection 4.2](#). This is in terms of reducing energy costs subject to compliance with constraints (i.e., all RL agents have the same [Equation 11h](#)). We also include random agents to further study the effectiveness of the safety layers and to serve as a minimal learning benchmark. The linear MPC from [Ceusters et al.](#) [4] is not included here, as the constraints can be formulated directly in the method. Note that any uncertainty (e.g., from demands, prices, or renewables) is inherently handled by the RL agents in accordance with the *expectation*  $E\{\cdot\}$  in [Equation 4a](#). The experiments are carried out on a local machine that has an Intel® Core™ i5-8365U CPU @1.6GHz, 16 GB of RAM, and an SSD.

### 5. Results and discussion

The simulated performance, in terms of minimisation of energy costs subject to the fulfilment of the constraints, is shown in [Figure 4](#) and [Figure 5](#), with their numerical values after training (at time step 350,400) in [Table 3](#) and before training (at time step 0) in [Table 4](#). The objective values (i.e., the rewards using [Equation 11h](#), which has both  $L_{cost}^t$  and  $L_{comfort}^t$ ) are shown both in absolute values and relative to the *vanilla* RL benchmark (i.e., without a safety layer). The constraint tolerance we define here as the difference between the *true* constraints (i.e., observed after executing the control actions in the more detailed simulation environment) and the *modelled* constraints in the safety layer (i.e., computed in the safety layer itself, which is only *believed* to be true – see [Table 2](#) and [Figure 6](#)). While, in principle, this is a calculation for the complete constraint set, we focus here on the most limiting constraint being the thermal energy balance of [Equation 9d](#). Note that, this is only for the constraint tolerance metric and that [Equation 8a](#) till [Equation 8e](#) are still part of the mixed-integer quadratic program in the safety layer (this as their influence on the metric over the complete constraint set is marginal and can therefore be neglected). The constraint tolerance metric is then shown as the mean average error normalised to the thermal demand range (NMAE) and shown as the normalised sum (NSUM) over all evaluation time steps (i.e., 0% would then

mean perfect thermal energy balance and thus constraint fulfilment, over all evaluation time steps). We again want to emphasise the lack of a simulated control system (as discussed in subsection 4.2), resulting in an NSUM of approximately 5%, as determined by Ceusters *et al.* [5] in the same simulated case study, and the deliberately more detailed simulation model itself (to better mimic a real case study).

**Table 3.** 5-run average policy performance with a training budget of 10 years worth of time steps per run (i.e., 350,400 time steps per run)

EMS algorithm	Objective value		Constraint tolerance	
	absolute	relative	NMAE	NSUM
Unsafe TD3	-5,080	100.0%	8.1%	22.3%
OptLayer [6] TD3	-4,915	103.4%	<b>2.3%</b>	<b>6.1%</b>
SafeFallback [5] TD3	-4,943	102.8%	3.9%	9.9%
OptLayerPolicy TD3	-4,924	103.2%	2.4%	6.2%
GreyOptLayerPolicy TD3	<b>-4,844</b>	<b>104.9%</b>	2.5%	6.5%

These results show that our GreyOptLayerPolicy method outperforms all other benchmarks after training (104.9%), yet with a slightly worse constraint tolerance (2.5%) than the original OptLayer method (2.3%). Also, the initial utility of both of our proposed methods is significantly higher (92.4% and 92.2%) compared to OptLayer (86.1%), as initially, they use the SafeFallback policy  $\pi^{safe}$  itself (97.2%) – due to exceeding the set threshold  $h_{safe}$  in algorithm 1. All safety layer methods are, as intended, significantly safer than the unconstrained *vanilla* TD3 benchmark, which has an initial NMAE of 56.5% and reaches 8.1% under the consequence of the  $L_{comfort}^t$  term in Equation 11h. The higher constraint tolerance of the original SafeFallback method itself can be explained by the fact that it is not capable of handling equality constraints [5] (as otherwise the constraint *check* would seldom be passed). The constraint tolerances of the other safety layer methods are of the same order of magnitude, both before and after training – all in line with the NMAE of the constraint functions themselves (Table 2 and Figure 6). The small difference before training between OptLayerPolicy and GreyOptLayerPolicy can be explained by the remaining variance in the results, as at this stage they both use the (same) nominal constraints.

**Table 4.** 5-run average policy performance before any training (i.e., the initial utility)

EMS algorithm	Objective value		Constraint tolerance	
	absolute	relative	NMAE	NSUM
Unsafe Random	-14,223	35.7%	56.5%	146.0%
OptLayer [6] Random	-5,900	86.1%	3.1%	8.0%
SafeFallback [5] Random	-5,331	95.3%	2.7%	7.0%
SafeFallback [5] ( $\pi^{safe}$ )	<b>-5,228</b>	<b>97.2%</b>	<b>2.4%</b>	<b>6.3%</b>
OptLayerPolicy Random	-5,499	92.4%	2.9%	7.4%
GreyOptLayerPolicy Random	-5,512	92.2%	2.8%	7.2%

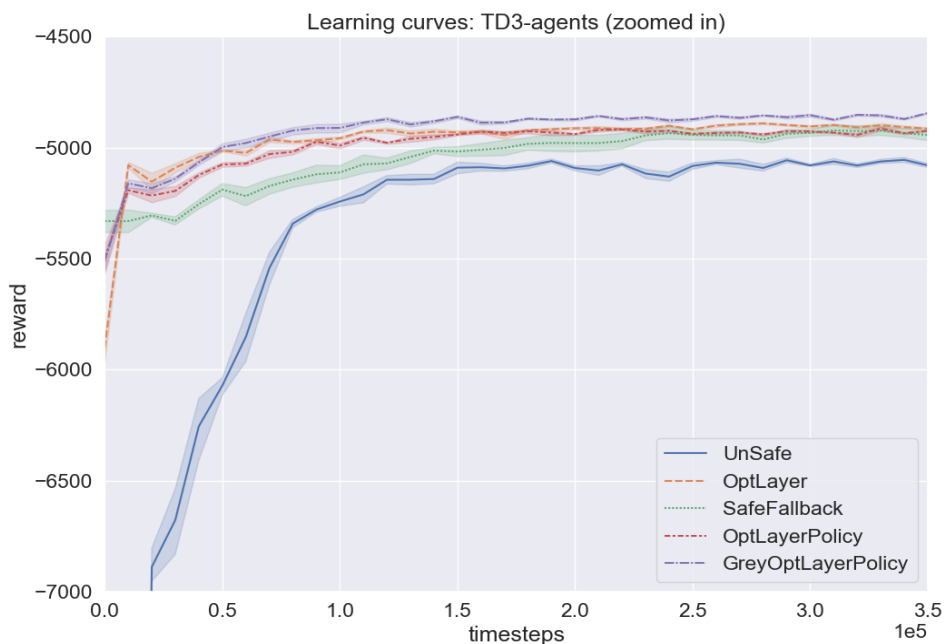


**Figure 4.** 5-run average learning curves with a training budget of 10 years worth of time steps per run (i.e., 350,400 time steps per run). Note that the y-axis is zoomed in (see [Figure B.1](#) in [Appendix B](#) for the zoomed-out version)

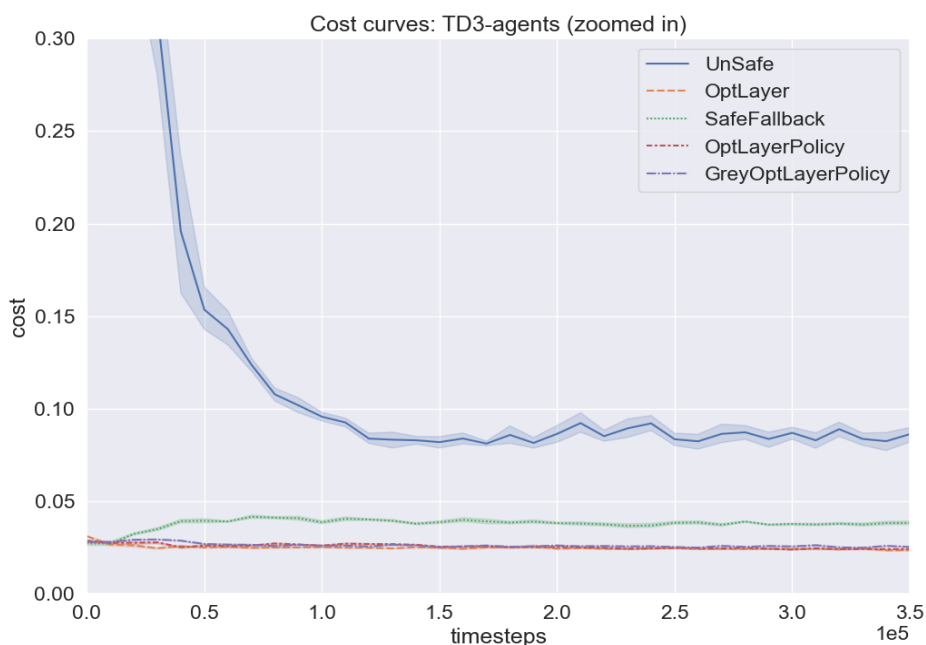


**Figure 5.** 5-run average cost curve (i.e., normalised mean absolute error) with a training budget of 10 years worth of time steps per run (i.e., 350,400 time steps per run). Note that the y-axis is zoomed in (see [Figure B.2](#) in [Appendix B](#) for the zoomed-out version).

In the learning curves of the TD3 agents (Figure 4) we observe a steep initial learning rate (except for the original SafeFallback method), low variance and stable performance with an increasing amount of interactions with its environment. As already reported here, we observe that our OptLayerPolicy and GreyOptLayerPolicy have a significantly higher initial utility compared to the original OptLayer and *vanilla* Unsafe approach. This, again, is due to the additional *a priori* expert knowledge in the form of the safe fallback policy  $\pi^{safe}$  and in the form of the constraint functions themselves (which is also true for the OptLayer approach compared to the unsafe *vanilla* RL agent). The GreyOptLayerPolicy algorithm surpasses OptLayerPolicy just after  $\approx 20,000$  time steps (7 months) and OptLayer after  $\approx 50,000$  time steps (17 months). The original SafeFallback method gets quickly surpassed by all other safety layer methods (all around 5,000 time steps, e.g. after 5,155 time steps for the GreyOptLayerPolicy method).

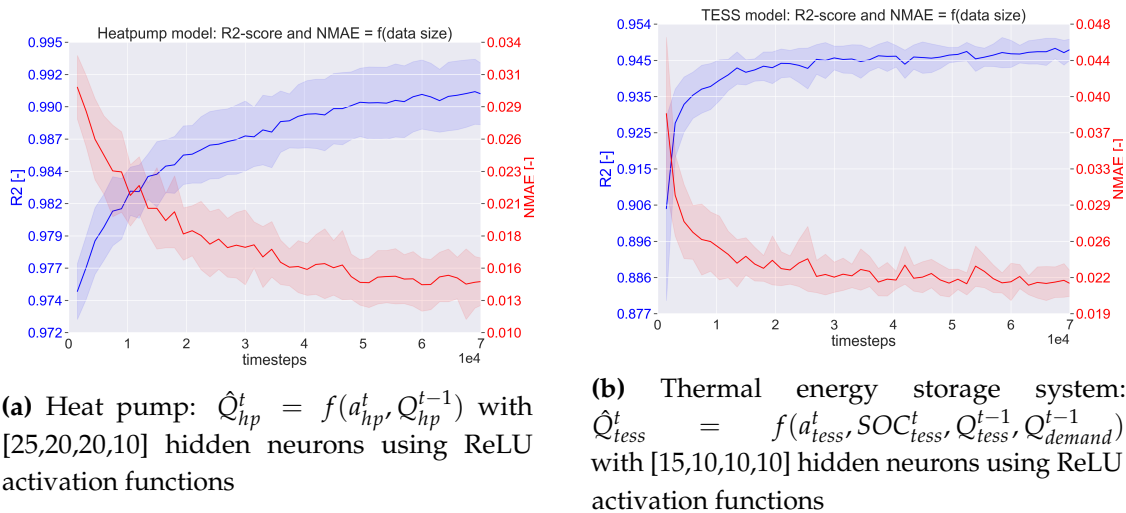


**Figure 6.** Safety layer: total (nominal and unknown component, i.e. Equation 7) modelling metrics for the first 2 years' worth of data, while interacting with the environment. The Mean Absolute Error is normalised by range (right-hand y-axis).

In the cost curves of the TD3 agents (Figure 5) we observe a relatively constant constraint tolerance when using a safety layer (although, in the GreyOptLayerPolicy method, the constraint functions themselves also improve – as can be seen in Figure 6 and compared to Table 2, i.e. starting from 3.64% NMAE for the heat pump to 1.14% and from 4.18% for the thermal energy storage system to 2.21%), which can be explained by the fact that energy fulfilment is conflicting with the energy cost minimisation objective (i.e., without a thermal demand fulfilment constraint, all thermal production would be turned off as these technical units consume and thus cost energy). The energy-minimising RL agents, therefore, push the multi-energy system to the respective limit of their energy balancing constraints (and thus exploit the nominal and remaining modelling error of the constraint functions themselves). The unconstrained *vanilla* TD3 benchmark does have a significant drop in its constraint tolerance under the consequence of the  $L_{comfort}^t$  term in Equation 11h (which has far less impact when using a safety layer, yet still results in a slightly better constraint tolerance for OptLayer and OptLayerPolicy - as its predicted actions  $\tilde{a}$  are more "falsely

considered" to be unsafe giving the additional cost  $z$  and a higher  $L_{comfort}^t$ , which essentially is an overcompensation towards safer actions). As mentioned before, the higher constraint tolerance of the original SafeFallback method itself can be explained by the fact that it is not capable of handling equality constraints (since otherwise the constraint *check* would seldom be passed), forcing a relaxation of the thermal energy balance constraint.

## 6. Conclusion

This paper presented a novel model-free safe RL approach of the following *combined* characteristics: (i) providing hard-constraints satisfaction guarantees (ii) while decoupled from the RL (as a Markov Decision Process) formulation, (iii) both during training a (near) optimal policy (involving exploratory and exploitative steps) as well as during the deployment of any policy (e.g., offline pre-trained RL agents) and (iv) this while learning uncertain constraint components and safely improving the policy with high sample efficiency, and (v) starting from an increased initial utility, to (vi) demonstrate for the energy management of multi-energy systems.

We conclude that, while special attention is required to introduce surrogate functions into the optimisation problem, the GreyOptLayerPolicy method is the most advantageous due to both the increase of its initial utility (92.2% compared to 86.1% for OptLayer) *and* the ability to self-improve its constraints (1.14% NMAE starting from 3.64% for the heat pump and 2.21% NMAE starting from 4.18% for the thermal energy storage system), leading to better policies (104.9% compared to 103.4% for OptLayer). This is despite the initial utility for the GreyOptLayerPolicy method being lower than the SafeFallback method, as this gets quickly surpassed (after 5,155 time steps) due to the high sample efficiency of GreyOptLayerPolicy and also despite the general reliance on the availability of nominal constraints and a safe fallback policy. Finally, we propose the following directions for future work:

- Ensuring the robustness of RL-based energy management systems against faulty and noisy measurements or observations while utilising the capabilities of online hyperparameter optimisation methods - wherein the hyperparameters of the RL agent are dynamically tuned during training.
- Reduce computational complexity of the safety layer when using surrogate constraint functions or parameters so that more detailed function approximation architectures can be used (e.g., more neurons and layers in an ANN).
- Verification of the proposed safety layers in a controlled laboratory environment, using inherently unsafe control methods (e.g., random and RL agents, as in this work).

## 7. Acknowledgement

This research has received equal support from ABB n.v. and the Flemish Agency for Innovation and Entrepreneurship (VLAIO) under grant HBC.2019.2613.

### CRedit authorship contribution statement

**Glenn Ceusters:** Conceptualisation, Methodology, Software, Validation, Formal analysis, Resources, Data curation, Writing - original draft, Visualisation, Funding acquisition;  
**Muhammad Andy Putratama:** Conceptualisation, Writing - review and editing, Supervision;

**Rüdiger Franke:** Supervision; **Ann Nowé:** Writing - review and editing, Supervision; **Maarten Messaie:** Supervision.

## Appendix A Time series visualisations

In this first appendix, we show time series visualisation samples of 1 week using the self-discovered control policies. The plots and their description of the benchmarks (i.e., `UnSafe`, `OptLayer` and `SafeFallback`) are not repeated here, as they can be found in [Ceusters et al. \[5\]](#). Our first observation is that the initial policy of both `OptLayerPolicy` ([Figure A.1](#)) and `GreyOptLayerPolicy` ([Figure A.3](#)) are very similar. This is, at this stage, they have the same (nominal) constraints, and occasionally the predicted actions,  $\tilde{a}$ , are close enough to the feasible solution space (calculated using [Equation 6](#)) so that they are minimally corrected and thus do not exceed the given threshold  $h_{safe}$ . As intended, most of the time this threshold is exceeded, and thus the safe fallback policy  $\pi_{safe}$  is used – in accordance with [algorithm 1](#).

When analysing the policies of the TD3 agents, after safely training them (i.e., [Figure A.2](#) and [Figure A.4](#)), we observe that both continue to have a low constraint tolerance, as expected. However, the `GreyOptLayerPolicy` policy is slightly better at using the heat pump when electricity prices are low, producing electricity with the CHP and charging the TESS simultaneously when electricity prices are high, and vice versa. Hence, it is better at minimising energy costs. In both cases, however, the BESS is underutilised, i.e., it fails to learn to charge the BESS when electricity prices are low and discharging the BESS when prices are high. This underuse of the BESS was also reported in previous work (e.g., [Ceusters et al. \[4\]](#) and [Ceusters et al. \[5\]](#)), which will require revisiting the state-space formulation ([Equation 11a](#)) and the consideration of specific reward shaping in [Equation 11h](#).

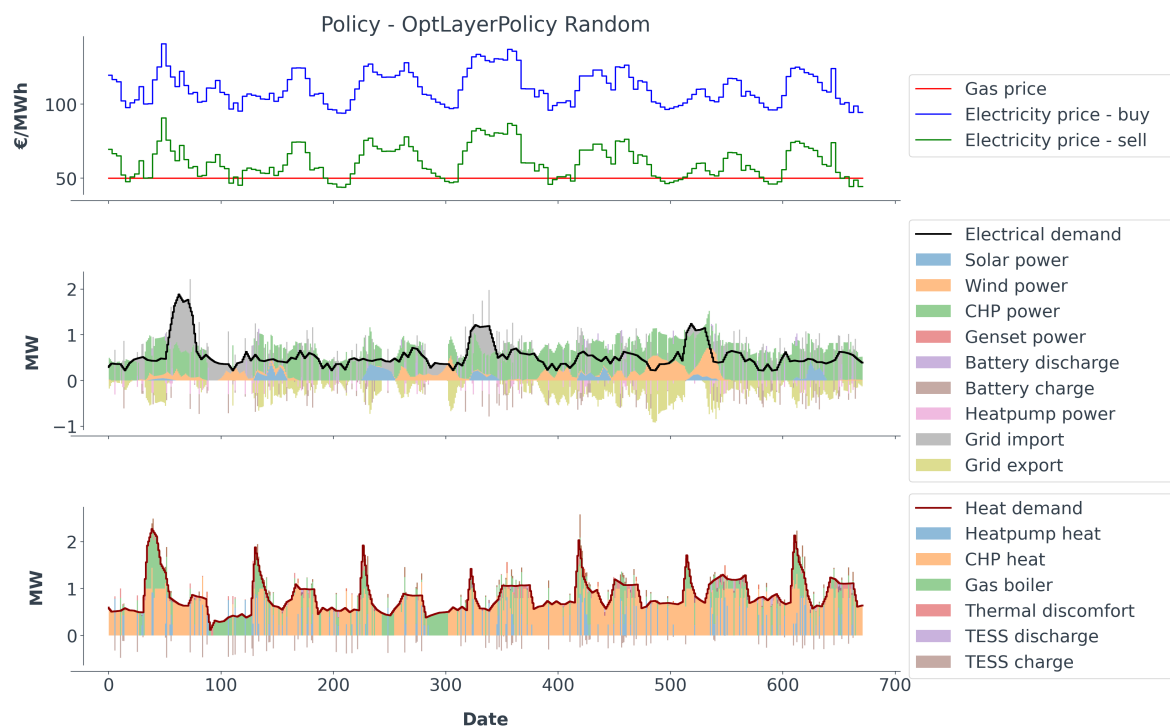


**Figure A.1.** Policy visualisation: `OptLayerPolicy` random (or TD3 before training)



Figure A.2. Policy visualisation: OptLayerPolicy TD3 (after safe training)

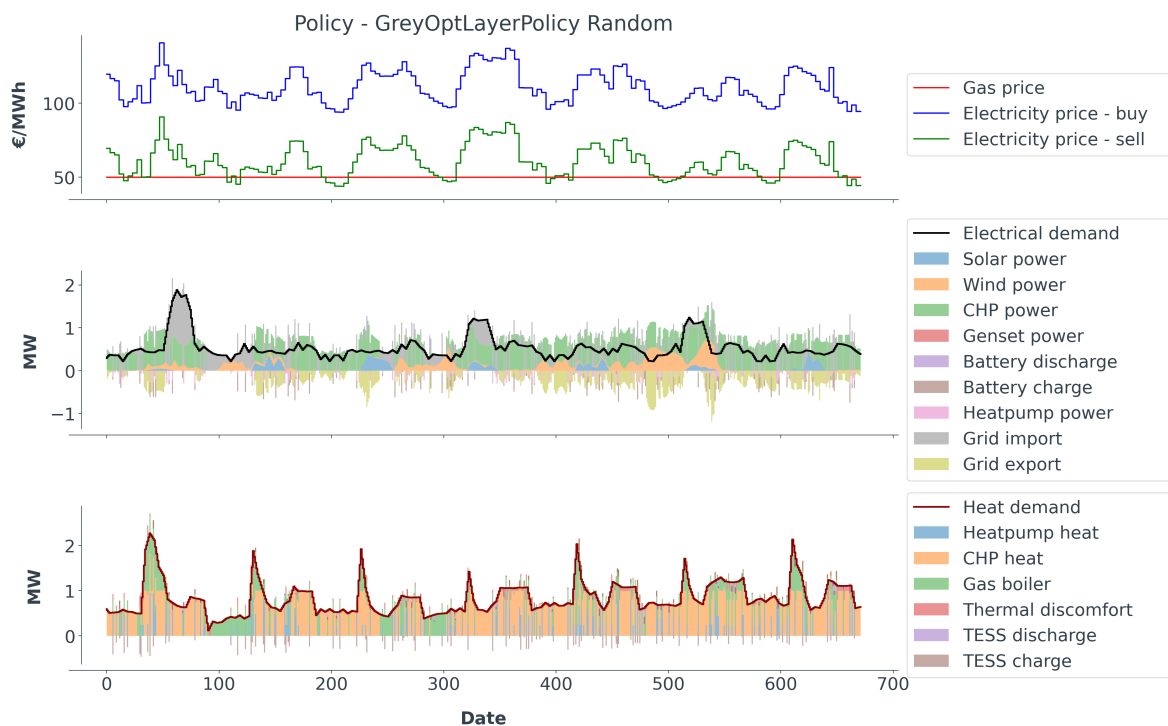
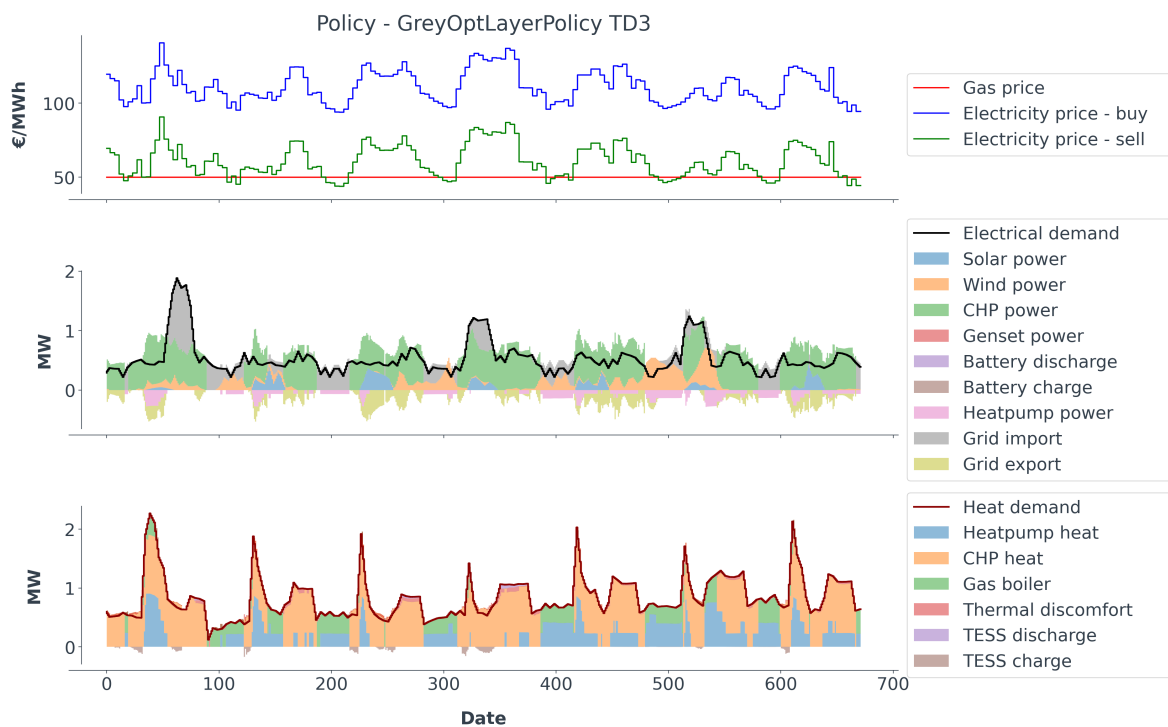


Figure A.3. Policy visualisation: GreyOptLayerPolicy random (or TD3 before training)



**Figure A.4.** Policy visualisation: GreyOptLayerPolicy TD3 (after safe training)

## Appendix B Learning and cost curves: zoomed out

This appendix shows the zoomed-out learning and cost curves of the TD3 agents so that all curves are fully visible, i.e., so that the UnSafe curves are visible for all time steps.

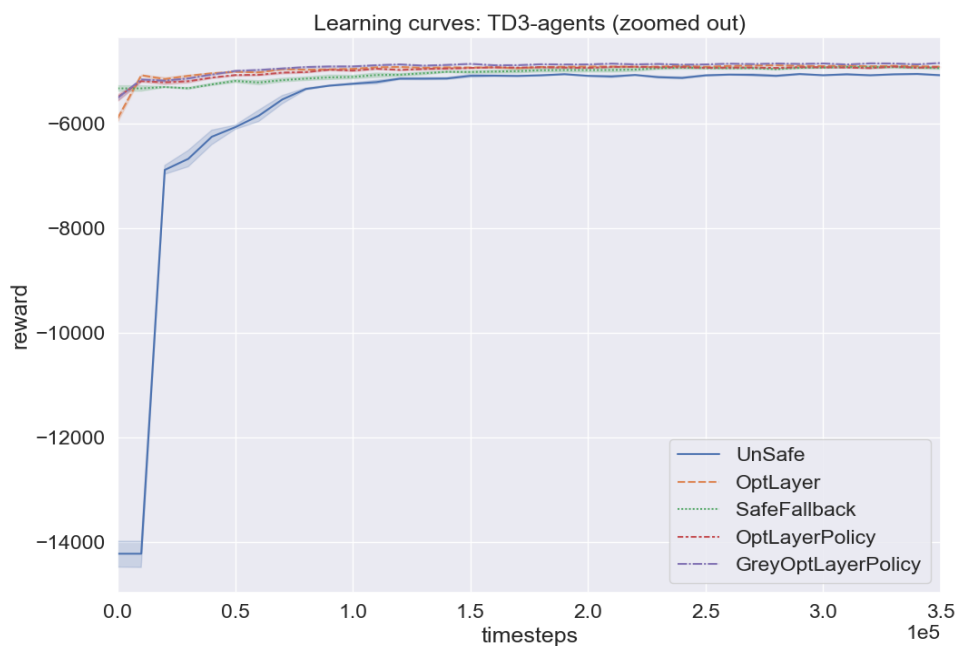


**Figure B.1.** 5-run average learning curves with a training budget of 10 years worth of time steps per run (i.e., 350,400 time steps per run). Note that the zoomed-in version is [Figure 4](#).

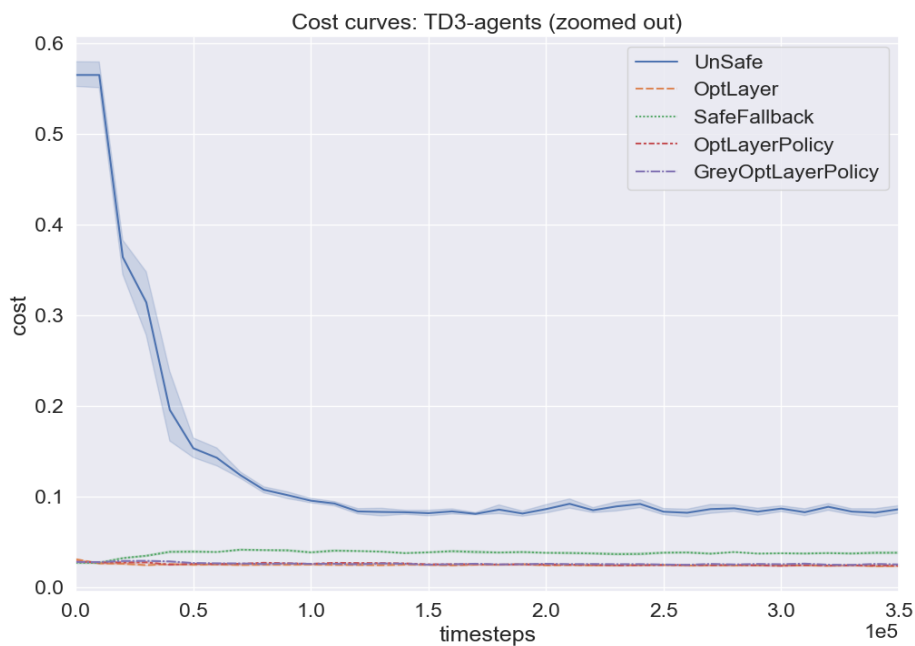


**Figure B.2.** 5-run average cost curve (i.e., normalised mean absolute error) with a training budget of 10 years worth of time steps per run (i.e., 350,400 time steps per run). Note that the zoomed-in version is [Figure 5](#).

### Appendix C Pseudocode and hyperparameters of TD3

---

**Algorithm 4:** Twin Delayed DDPG (TD3) [39]

---

- 1 Input: initial policy parameters  $\theta$ , Q-function parameters  $\phi_1, \phi_2$ , empty replay buffer  $\mathcal{D}$
- 2 Set target parameters equal to main parameters  $\theta_{target} \leftarrow \theta, \theta_{target,1} \leftarrow \theta_1, \theta_{target,2} \leftarrow \theta_2$
- 3 **repeat**
- 4   Observe state  $s$  and select action  $a = \text{clip}(\mu_\theta(s) + \epsilon, a_{Low}, a_{High})$ , where  $\epsilon \sim \mathcal{N}$
- 5   Execute  $a$  in the environment
- 6   Observe next state  $s'$ , reward  $r$  and done signal  $d$  to indicate whether  $s'$  is terminal
- 7   Store  $(s, a, r, s', d)$  in replay buffer  $\mathcal{D}$
- 8   If  $s'$  is terminal, reset environment state
- 9   **if it's time to update then**
- 10    **for**  $j$  in range(however many updates) **do**
- 11      Randomly sample a batch of transitions,  $B = \{(s, a, r, s', d)\}$  from  $\mathcal{D}$
- 12      Compute target actions

$$a'(s') = \text{clip}(\mu_{\theta_{target}}(s') + \text{clip}(\epsilon, -c, c), a_{Low}, a_{High}), \quad \epsilon \sim \mathcal{N}(0, \sigma)$$

- 13    Compute targets

$$y(r, s', d) = r + \gamma(1 - d) \min_{i=1,2} Q_{\phi_{target,i}}(s', a'(s'))$$

- 14    Update Q-function by one step of gradient descent using

$$\nabla_{\phi_i} \frac{1}{|B|} \sum_{(s,a,r,s',d) \in B} (Q_{\phi_i}(s, a) - y(r, s', d))^2 \quad \text{for } i = 1, 2$$

- 15    **if**  $j \bmod \text{policy\_delay} = 0$  **then**
- 16      Update policy by one step of gradient ascent using

$$\nabla_{\theta} \frac{1}{|B|} \sum_{s \in B} Q_{\phi_1}(s, \mu_\theta(s))$$

- 17    Update target networks with

$$\begin{aligned} \phi_{target,i} &\leftarrow \rho \phi_{target,i} + (1 - \rho) \phi_i & \text{for } i = 1, 2 \\ \theta_{target} &\leftarrow \rho \theta_{target} + (1 - \rho) \theta \end{aligned}$$

- 18    **end if**
  - 19    **end for**
  - 20    **end if**
  - 21 **until** convergence
-

**Table C.1.** TD3 hyperparameters. The parameters from the *vanilla* Unsafe agent are the result of an optimisation study from [Ceusters et al. \[4\]](#), while the others are the resulting SafeFallback parameters from [Ceusters et al. \[5\]](#)

Hyperparameters: TD3	Unsafe	OptLayer OptLayerPolicy GreyOptLayerPolicy
gamma	0.9	0.7
learning_rate	0.0003833	0.000583
batch_size	100	16
buffer_size	1e5	1e6
train_freq	2e3	1e0
gradient_steps	2e3	1e0
noise_type	normal	normal
noise_std	0.329	0.183

## Appendix D Run-time statistics

The experiments are performed on a local machine that has an Intel® Core™ i5-8365U CPU @1.6GHz, 16 GB of RAM, and an SSD. Over a yearly simulation, the following run-time statistics per simulated time step (with a control horizon of 15 min) are observed.

**Table D.1.** Run-time statistics *after* training (i.e., pure policy execution)

Optimal controller	min	mean	std	max	total
Unsafe TD3	0,032 s	0,053 s	0,009 s	0,270 s	1.858 s
Unsafe Random	0,029 s	0,046 s	0,008 s	0,124 s	1.630 s
OptLayer TD3	0,211 s	0,291 s	0,036 s	0,976 s	10.204 s
OptLayer Random	0,177 s	0,254 s	0,042 s	2,256 s	8.917 s
SafeFallback TD3	0,042 s	0,061 s	0,007 s	0,189 s	2.134 s
SafeFallback Random	0,038 s	0,046 s	0,007 s	0,492 s	1.608 s
SafeFallback ( $\pi^{safe}$ )	0,038 s	0,050 s	0,010 s	0,190 s	1.738 s
OptLayerPolicy TD3	0,202 s	0,257 s	0,023 s	1,259 s	9.008 s
OptLayerPolicy Random	0,177 s	0,222 s	0,028 s	2,897 s	7.783 s
GreyOptLayerPolicy TD3	1,442 s	1,944 s	0,378 s	10,066 s	68.106 s
GreyOptLayerPolicy Random	1,436 s	1,918 s	0,361 s	6,504 s	67.222 s

The maximum run-time per time step never exceeds the control horizon of 15 minutes, as the deployment of the algorithm would then otherwise be considered infeasible with the given hardware. We observe that both the Unsafe and SafeFallback approaches have the fastest run-time, as they do not have a mathematical program to solve. However, we have argued that using a *vanilla* RL agent (i.e., without any safety measures) is not realistic in safety-critical environments and is given here only for completeness. We have also argued that the SafeFallback approach is not capable of handling equality constraints, resulting in a higher constraint tolerance and is seen as a major drawback of the original method. As expected, the run-time of the OptLayer and OptLayerPolicy approaches are in the same order of magnitude, as both involve solving a mixed-integer quadratic program (MIQP) in order to compute the closest feasible action and the distance of the predicted action,  $\tilde{a}$ , to the feasible solution space. Finally, we observe that the GreyOptLayerPolicy approach has the slowest run-time, which in turn hurts its scalability. This is because the surrogate functions that are used to learn the uncertain constraint components are converted within the gradient descent

optimisation framework of GEKKO to allow for an exact solution. As proposed in future work, other methods of integrating surrogate functions should be explored to reduce computational complexity.

## References

1. Fabrizio, E.; Filippi, M.; Virgone, J. Trade-off between environmental and economic objectives in the optimization of multi-energy systems. *Building Simulation* **2009**, *2*, 29–40. doi:10.1007/S12273-009-9202-4.
2. Engell, S. Feedback control for optimal process operation. *Journal of Process Control* **2007**, *17*, 203–219. doi:10.1016/J.PROCONT.2006.10.011.
3. Görges, D. Relations between Model Predictive Control and Reinforcement Learning. *IFAC-PapersOnLine* **2017**, *50*, 4920–4928. doi:10.1016/j.ifacol.2017.08.747.
4. Ceusters, G.; Rodríguez, R.C.; García, A.B.; Franke, R.; Deconinck, G.; Helsen, L.; Nowé, A.; Messagie, M.; Camargo, L.R. Model-predictive control and reinforcement learning in multi-energy system case studies. *Applied Energy* **2021**, *303*, 117634. doi:10.1016/j.apenergy.2021.117634.
5. Ceusters, G.; Camargo, L.R.; Franke, R.; Nowé, A.; Messagie, M. Safe reinforcement learning for multi-energy management systems with known constraint functions. *Energy and AI* **2023**, *12*, 100227. doi:10.1016/J.EGYAI.2022.100227.
6. Pham, T.H.; De Magistris, G.; Tachibana, R. OptLayer - Practical Constrained Optimization for Deep Reinforcement Learning in the Real World. *Proceedings - IEEE International Conference on Robotics and Automation* **2018**, pp. 6236–6243. doi:10.1109/ICRA.2018.8460547.
7. Cao, D.; Hu, W.; Zhao, J.; Zhang, G.; Zhang, B.; Liu, Z.; Chen, Z.; Blaabjerg, F. Reinforcement Learning and Its Applications in Modern Power and Energy Systems: A Review. *Journal of Modern Power Systems and Clean Energy* **2020**, *8*, 1029–1042. doi:10.35833/MPCE.2020.000552.
8. Yang, T.; Zhao, L.; Li, W.; Zomaya, A.Y. Reinforcement learning in sustainable energy and electric systems: a survey. *Annual Reviews in Control* **2020**, *49*, 145–163. doi:10.1016/J.ARCONTROL.2020.03.001.
9. Perera, A.T.; Kamalaruban, P. Applications of reinforcement learning in energy systems. *Renewable and Sustainable Energy Reviews* **2021**, *137*, 110618. doi:10.1016/J.RSER.2020.110618.
10. Zhou, Y. Advances of machine learning in multi-energy district communities– mechanisms, applications and perspectives. *Energy and AI* **2022**, *10*, 100187. doi:10.1016/J.EGYAI.2022.100187.
11. Petrushev, A.; Putratama, M.A.; Rigo-Mariani, R.; Debusschere, V.; Reignier, P.; Hadjsaid, N. Reinforcement learning for robust voltage control in distribution grids under uncertainties. *Sustainable Energy, Grids and Networks* **2023**, *33*, 100959. doi:10.1016/J.SEGAN.2022.100959.
12. Zhou, Y.; Ma, Z.; Zhang, J.; Zou, S. Data-driven stochastic energy management of multi energy system using deep reinforcement learning. *Energy* **2022**, *261*, 125187. doi:10.1016/J.ENERGY.2022.125187.
13. Pu, Y.; Wang, S.; Yang, R.; Yao, X.; Li, B. Decomposed Soft Actor-Critic Method for Cooperative Multi-Agent Reinforcement Learning. *arXiv* **2021**.
14. Zhu, D.; Yang, B.; Liu, Y.; Wang, Z.; Ma, K.; Guan, X. Energy Management Based on Multi-Agent Deep Reinforcement Learning for A Multi-Energy Industrial Park. *Applied Energy* **2022**, *311*, 118636. doi:10.1016/j.apenergy.2022.118636.
15. Ahrarinouri, M.; Rastegar, M.; Karami, K.; Seifi, A.R. Distributed reinforcement learning energy management approach in multiple residential energy hubs. *Sustainable Energy, Grids and Networks* **2022**, *32*, 100795. doi:10.1016/J.SEGAN.2022.100795.
16. Jendoubi, I.; Bouffard, F. Data-driven sustainable distributed energy resources' control based on multi-agent deep reinforcement learning. *Sustainable Energy, Grids and Networks* **2022**, *32*, 100919. doi:10.1016/J.SEGAN.2022.100919.
17. Sun, B.; Song, M.; Li, A.; Zou, N.; Pan, P.; Lu, X.; Yang, Q.; Zhang, H.; Kong, X. Multi-objective solution of optimal power flow based on TD3 deep reinforcement learning algorithm. *Sustainable Energy, Grids and Networks* **2023**, *34*, 101054. doi:10.1016/J.SEGAN.2023.101054.
18. García, J.; Fernández, F. A comprehensive survey on safe reinforcement learning, 2015.

19. Feng, J.; Wang, H.; Yang, Z.; Chen, Z.; Li, Y.; Yang, J.; Wang, K. Economic dispatch of industrial park considering uncertainty of renewable energy based on a deep reinforcement learning approach. *Sustainable Energy, Grids and Networks* **2023**, *34*, 101050. doi:10.1016/J.SEGAN.2023.101050.
20. Zhu, D.; Yang, B.; Liu, Q.; Ma, K.; Zhu, S.; Ma, C.; Guan, X. Energy trading in microgrids for synergies among electricity, hydrogen and heat networks. *Applied Energy* **2020**, *272*, 115225. doi:10.1016/J.APENERGY.2020.115225.
21. Zhu, D.; Yang, B.; Ma, C.; Wang, Z.; Zhu, S.; Ma, K.; Guan, X. Stochastic gradient-based fast distributed multi-energy management for an industrial park with temporally-coupled constraints. *Applied Energy* **2022**, *317*, 119107. doi:10.1016/J.APENERGY.2022.119107.
22. Zou, Y.; Xu, Y.; Feng, X.; Nguyen, H.D. Peer-to-Peer Transactive Energy Trading of a Reconfigurable Multi-Energy Network. *IEEE Transactions on Smart Grid* **2023**, *14*, 2236–2249. doi:10.1109/TSG.2022.3223378.
23. Zou, Y.; Xu, Y.; Zhang, C. A Risk-Averse Adaptive Stochastic Optimization Method for Transactive Energy Management of a Multi-Energy Microgrid. *IEEE Transactions on Sustainable Energy* **2023**, *14*, 1599–1611. doi:10.1109/TSTE.2023.3240184.
24. Brunke, L.; Greeff, M.; Hall, A.W.; Yuan, Z.; Zhou, S.; Panerati, J.; Schoellig, A.P. Safe Learning in Robotics: From Learning-Based Control to Safe Reinforcement Learning. *Annual Review of Control, Robotics, and Autonomous Systems* **2021**, *5*. doi:10.1146/annurev-control-042920-020211.
25. McKinnon, C.D.; Schoellig, A.P. Context-aware Cost Shaping to Reduce the Impact of Model Error in Receding Horizon Control. *Proceedings - IEEE International Conference on Robotics and Automation* **2020**, pp. 2386–2392. doi:10.1109/ICRA40945.2020.9197521.
26. Bharadhwaj, H.; Kumar, A.; Rhinehart, N.; Levine, S.; Shkurti, F.; Garg, A. Conservative Safety Critics for Exploration. International Conference on Learning Representations, 2021.
27. Lopez, B.T.; Slotine, J.J.E.; How, J.P. Robust Adaptive Control Barrier Functions: An Adaptive and Data-Driven Approach to Safety. *IEEE Control Systems Letters* **2021**, *5*, 1031–1036. doi:10.1109/LCSYS.2020.3005923.
28. Sutton, R.S.; Barto, A.G. *Reinforcement learning: An introduction*; MIT press, 2018.
29. Gunnell, L.L.; Manwaring, K.; Lu, X.; Reynolds, J.; Vienna, J.; Hedengren, J. Machine Learning with Gradient-Based Optimization of Nuclear Waste Vitrification with Uncertainties and Constraints. *Processes* **2022**, *10*, 2365. doi:10.3390/pr10112365.
30. Beal, L.; Hill, D.; Martin, R.; Hedengren, J. GEKKO Optimization Suite. *Processes* **2018**, *6*, 106. doi:10.3390/pr6080106.
31. Mattsson, S.E.; Elmqvist, H.; Otter, M. Physical system modeling with Modelica. *Control Engineering Practice*. Pergamon, 1998, Vol. 6, pp. 501–510. doi:10.1016/S0967-0661(98)00047-1.
32. Gräber, M.; Fritzsche, J.; Tegethoff, W. From system model to optimal control - A tool chain for the efficient solution of optimal control problems. Proceedings of the 12th International Modelica Conference, Prague, Czech Republic, May 15-17, 2017. Linköping University Electronic Press, 2017, Vol. 132, pp. 249–254. doi:10.3384/ecp17132249.
33. Brockman, G.; Cheung, V.; Pettersson, L.; Schneider, J.; Schulman, J.; Tang, J.; Zaremba, W. OpenAI Gym. *arXiv* **2016**.
34. Pedregosa FABIANPEDREGOSA, F.; Michel, V.; Grisel OLIVIERGRISEL, O.; Blondel, M.; Prettenhofer, P.; Weiss, R.; Vanderplas, J.; Cournapeau, D.; Pedregosa, F.; Varoquaux, G.; Gramfort, A.; Thirion, B.; Grisel, O.; Dubourg, V.; Passos, A.; Brucher, M.; Perrot and Édouardand, M.; Duchesnay, a.; Duchesnay EDOUARDDUCHESNAY, F. Scikit-learn: Machine learning in Python. *jmlr.org Pedregosa, G Varoquaux, A Gramfort, V Michel, B Thirion, O Grisel, M Blondelthe Journal of machine Learning research, 2011•jmlr.org* **2011**, *12*, 2825–2830.
35. Andersson, C.; Akesson, J.; Fuhrer, C. PyFMI: A Python Package for Simulation of Coupled Dynamic Models with the Functional Mock-up Interface. Technical Report 2, Lund University, 2016.
36. Drgoňa, J.; Arroyo, J.; Cupeiro Figueroa, I.; Blum, D.; Arendt, K.; Kim, D.; Ollé, E.P.; Oravec, J.; Wetter, M.; Vrabie, D.L.; Helsen, L. All you need to know about model predictive control for buildings. *Annual Reviews in Control* **2020**, *50*, 190–232. doi:10.1016/j.arcontrol.2020.09.001.
37. Kingma, D.P.; Ba, J. Adam: A Method for Stochastic Optimization **2014**.

38. Raffin, A.; Hill, A.; Gleave, A.; Kanervisto, A.; Ernestus, M.; Dormann, N. Stable-Baselines3: Reliable Reinforcement Learning Implementations. *Journal of Machine Learning Research* **2021**, *22*, 1–8.
39. OpenAI. Twin Delayed DDPG — Spinning Up documentation, 2020.